JCTC Journal of Chemical Theory and Computation

Article

pubs.acs.org/JCTC

QM/QM Approach to Model Energy Disorder in Amorphous Organic Semiconductors

Pascal Friederich,[†] Velimir Meded,[†] Franz Symalla,[†] Marcus Elstner,[‡] and Wolfgang Wenzel*[,†]

[†]Institute of Nanotechnology (INT), Karlsruhe Institute of Technology (INT), Hermann-von-Helmholtz-Platz 1, 76344 Eggenstein-Leopoldshafen, Germany

[‡]Institute of Physical Chemistry (IPC), Karlsruhe Institute of Technology (KIT), Kaiserstraße 12, 76131 Karlsruhe, Germany

ABSTRACT: It is an outstanding challenge to model the electronic properties of organic amorphous materials utilized in organic electronics. Computation of the charge carrier mobility is a challenging problem as it requires integration of morphological and electronic degrees of freedom in a coherent methodology and depends strongly on the distribution of polaron energies in the system. Here we represent a QM/QM model to compute the polaron energies combining density functional methods for molecules in the vicinity of the polaron with computationally efficient density functional based tight binding methods in the rest of the environment. For seven widely used amorphous organic semiconductor materials, we show that the calculations are accelerated up to 1 order of magnitude without any loss in accuracy. Considering that the quantum chemical step is the efficiency bottleneck of a workflow to model the carrier mobility, these results are an important step toward accurate and efficient disordered organic semiconductors simulations, a prerequisite for accelerated materials screening and consequent component optimization in the organic electronics industry.

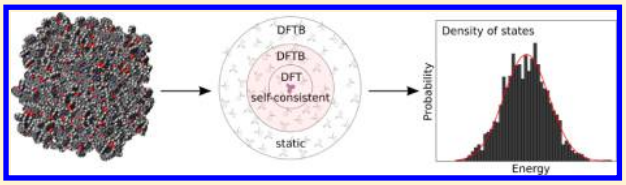

INTRODUCTION

Driven by both technological and fundamental interests, disordered small-molecule based organic semiconductor materials have been in focus of scientific research[1−3] and technological developments for many decades. Today these materials find applications in organic light emitting diodes (OLED) for both displays and lighting, organic photovoltaics (OPV), organic field effect transistors (OFET), etc., and have already been deployed in television sets, portable electronics,[4−7] and other devices of increasing complexity. Other applications, such as lightning or organic photovoltaics have not yet reached the level of competitiveness required for market entry. To further optimize these materials, development of reliable, predictive, and fast modeling methodologies to quantitatively simulate the electronic processes in the materials would be very helpful. In order to be predictive such methods need to elevate information on the molecular level via multiscale simulation workflows to the macroscopic scale, which may lead to better performing materials. There has been a plethora of different approaches, both (semi)analytical[8−11] and numerical,[12−14] to predict macroscopic quantities, such as intrinsic charge mobility, but to date no reliable modeling methodology covering a wide range of different materials has been developed.[15]

In many small molecule based materials, i.e. in the weak intermolecular coupling regime, the charge carrier mobility is well described by a polaron hopping model, where localized charges hop from one molecule in the system to the next. In the high temperature limit, an individual hopping process is usually[12,14,16] described as thermally activated transport in terms of Marcus theory:[17,18]

$$k_{if} = \frac{2\pi}{\hbar} |J_{if}|^2 \frac{1}{\sqrt{4\pi\lambda_{if} k_B T}} \exp\left(-\frac{(\lambda_{if} + \Delta G_{if})^2}{4\lambda_{if} k_B T} \right) \quad (1)$$

The dominant quantity, determining the Marcus hopping rate between two molecules is their Gibbs free energy difference ΔG_{if}. This can be approximated to the on-site energy difference ΔE_{if} of the molecules if entropic effects can be neglected which is the case in condensed phase materials. Two other contributions are the reorganization energy λ and the electronic coupling J_{if} between the molecules. The expression is crucial as it couples the microscopic degrees of freedom (energy disorder, hoping matrix elements) with the macroscopic degrees of freedom (temperature, external fields, etc.). To compute the relevant quantities from first-principles both a realistic morphology and accurate electronic structure calculations need to be employed. Solving the transport problem either with kinetic Monte Carlo approaches[9] or (semi)analytically[10] will then lead to an estimate of charge carrier mobilities.

In most models the main factor determining the charge carrier mobility is the width of the distribution of site energies, the energy disorder σ. In analytic models the dependence of the carrier mobility on the energy disorder is in general quadratic in the exponent.[9,19−21] The dependence on reorganization energy λ is weaker as it in general enters the exponent in linear fashion, but it is still stronger than the influence of hopping matrix elements J which enter the expression as a prefactor with quadratic rather than exponential dependence. However, one

Received: November 17, 2014
Published: January 7, 2015

 © 2015 American Chemical Society

DOI: 10.1021/ct501023n
J. Chem. Theory Comput. 2015, 11, 560−567

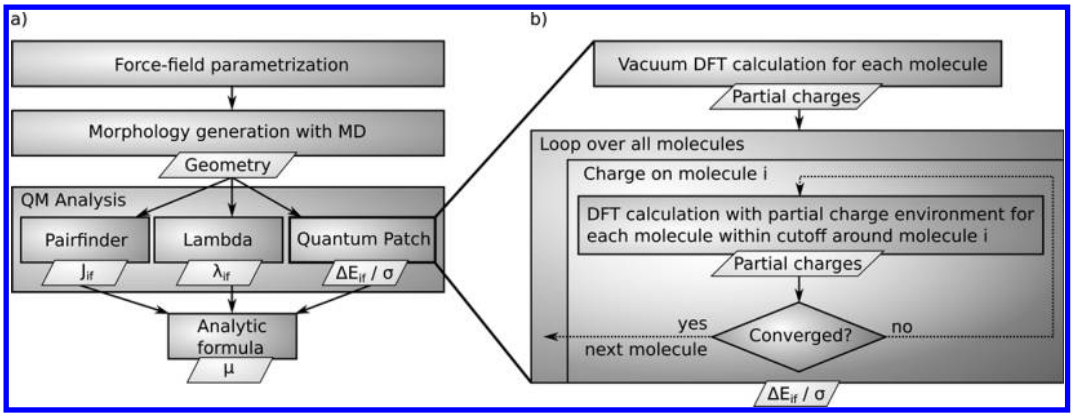

Figure 1. Schematic representation of the workflow: In a, the general workflow starting with morphology generation followed by quantum mechanical (QM) microscopic analysis and finishing by feeding the parameters obtained in QM step into the mobility expression. In b, details of the quantum patch protocol are being displayed. The most important component is the self-consistency loop over each molecule imbedded in partial charges of the environment performed until the partial charges of each molecule are converged with the single molecule total energy as convergence criterion.

should not forget that hopping matrix elements depend exponentially on the intermolecular distance and as such introduce an exponential contribution as far as the intermolecular distances are concerned. But, details of microscopic and morphology dependent characteristics e.g. molecular orientation and local environment have a very nontrivial impact on the hopping matrix element distribution, making it, in general, more complex than a simple distance dependent exponential function.

Investigation of lattice models with a Gaussian disorder distribution[9,11,22] typically leads to a dependence of the mobility on the width of the distribution σ and the inverse temperature as

$$\mu \propto \exp(-C(\beta\sigma)^2) \tag{2}$$

The factor C in the exponent in eq 2 depends on the details of the model used and the proximity of the percolation limit where current travels only through a single filament in the sample and on the degree of correlation in the disorder distribution sample and its topology. For a range of models C varies between the effective medium value of 0.25,[23] to roughly 0.44 for the percolation limit in the simple cubic lattice[11] and can reach values up to 0.69.[24] Given the strong dependence of the mobility on σ the calculation of the energetic disorder on a high level of accuracy is crucial for the prediction of charge carrier mobilities.

In the past the width of the energy disorder distribution was often estimated by fitting to experimental data assuming a particular model,[9,25] but this approach, as relying on fitting procedures, has obviously limited predictability. For this reason many groups have started to develop methods to explicitly calculate the energy differences between molecules on different level of theory.[14,15,26−28] From a microscopic perspective both intramolecular effects, i.e. distortions of the molecule induced by its environment, and polarization effects from the surrounding medium contribute to energy differences between different sites. In order to account for both effects we have developed a multiscale methodology, where we start with morphology generation for a sufficiently large sample of molecules using force field based methods[29] with a subsequent quantum mechanical,[28] density functional based[30−33] method for modeling polarons embedded in a disordered medium. This quantum mechanical computation of the polaron energy by the quantum patch method is by far the most numerically intensive step, comprising almost 200 000 DFT calculations on individual molecules in order to converge the relevant materials parameters, per studied system. Using state-of-the-art computational hardware, computing the disorder parameter for one charge species in a given system, can easily consume hundreds of thousands of CPU hours. For this reason the quantum patch step in its current form constitutes the computational bottleneck toward efficient in silico materials screening.

In this work, we investigate the possibility to combine fast semiempirical DFTB[34−36] calculations with the previously investigated quantum patch[28] method to test the trade-off between the speed and the accuracy and to explore the parametric space in search for the optimal approach by defining a number of cutoff shells and comparing the new combined approach with the full DFT[30] benchmark.

The paper is organized as follows: We first briefly explain the multiscale workflow and the steps (methods) therein. Then we investigate in detail the influence of various partitioning regions and cutoff radii in the quantum patch step. Afterward, we present the results of calculations of energetic disorder for these different methods and their impact on charge mobilities, compared to both the reference calculation (full DFT level as in ref 28).

METHODS

The multiscale workflow, see Figure 1, illustrates the steps that have to be performed in order to accurately interconnect the microscopic and macroscopic properties. The focus in this work is on the details in the energetic disorder calculations, but for completeness, we briefly go through the other steps first.

The amorphous morphologies were generated by mimicking rapid quenching of a liquid into an amorphous state at a temperature below the glass transition temperature of the material, a procedure that has previously been applied for the preparation of amorphous structures of OLED materials.[37−39] The molecular dynamics simulations were carried out using GROMACS6 program[29] using the general AMBER force field (GAFF)[40] with AM1-BCC partial charges[41,42] with periodic boundary conditions containing 300 molecules. The samples were periodically extended in order to generate sufficiently large morphologies for the polarization cutoffs. The central part of this extended morphologies contains several hundred pairs,

DOI: 10.1021/ct501023n
J. Chem. Theory Comput. 2015, 11, 560−567

which is sufficient for the reliable extraction of statistic quantities such as the energy disorder.

The recently proposed quantum patch method[28] is a parameter free protocol to calculate the electronic structure parameters in amorphous small molecules materials. In this method polarization contributions of the environment on the polaron energy which account for a significant fraction of the energetic disorder are taken into account in a self-consistent quantum embedding scheme. Because the entire sample is partitioned into sets of coupled molecules, the algorithm scales linearly with the number of hopping sites in the system. For each polaron the charge distribution within a neighbor shell of about 25 Å including about 100 molecules around the charged molecules needs to be equilibrated. In addition, the polarizing effect of the molecules within a cutoff radius of 60 Å including up to 3000 sites are taken into account in a static way. The self-consistent evaluation of the first shell is performed according to Figure 2.[28]

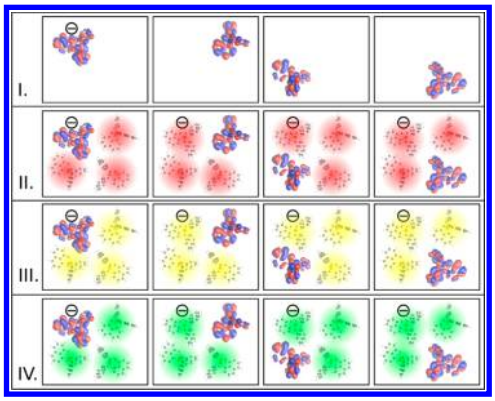

Figure 2. Schematic description of the algorithm used for the evaluation of the self-consistent region around a charged molecule. In the first step, vacuum partial charges for each molecule in this region are calculated (row I). An additional charge is assigned to the central molecule. Partial charges of this as well as of the neighboring molecules within a cutoff distance of 25 Å are self-consistently re-evaluated using a cloud of point charges that are iteratively improved until convergence in total energy of the charged molecule is reached,[28] where the charge cloud self-consistency cycle is represented by the changing cloud color from red to green (rows II to IV).

The partitioning of the system in a self-consistent and a static shell of molecules is motivated by the fact that the size of the induced polarization contribution diminishes with distance and that we are primarily interested on second order effect of the feedback of the induced polarization distribution on the central site. In the original quantum patch method the entire self-consistent shell was treated on the same level of accuracy as the charged molecule. As we are primarily interested in the energy of the latter, it may be possible to reduce the computational cost of the quantum patch approach by using more approximate methods on the former.

Here we therefore combine fast semiempirical DFTB[34] calculations for the neighbor shell and the second, unpolarized shell of molecules with the accurate DFT calculations for the charged central site into an de facto QM/QM approach. We note that in the quantum patch method the molecules interact with the environment in the QM shell via induced charges where the charge−dipole interaction is the leading contribution. If the molecular dipoles coming from DFTB are comparable to their DFT counterparts, replacement of expensive DFT at least for some parts of the system is plausible.

In order to investigate the interoperability and robustness of DFTB[34] and DFT combination in the quantum patch algorithm,[28] we split the molecular morphology in a number of regions as shown in Figure 3. We then compare this to the

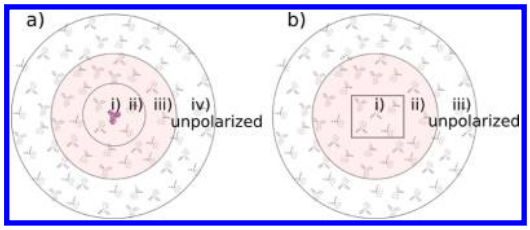

Figure 3. (a) Cutoff scheme for the full hybrid quantum patch method including explicit polarons. The colored regions are treated in a self-consistent way and contain about 100 molecules. Region i: charged molecule. Region ii: next nearest neighbor molecules within a cutoff distance of 12 Å. Region iii: neighbors within a distance of 25 Å. Region iv: unpolarized molecules within a cutoff distance of 60 Å (~3000 molecules). (b) Cutoff scheme for the polarized quantum patch method where the system is equilibrated without explicit additional charges. Region ii: molecules within a 25 Å cutoff distance around the central part i of the morphology. Each molecule in regions i and ii is treated in a self-consistent way.[28] The energy disorder is only extracted in the central region i to avoid edge-effects at the border between polarized and unpolarized regions. Region iii corresponds to region iv in method a.

performance of the quantum patch method where explicit additional charges ("polaron model") are included. The first approximation to the polaron model is the treatment of the molecules in area iv and iii with the faster semiempirical DFTB2 method (see Table 1). This will be referred to as the "hybrid large" method. The next approximation is the replacement of the DFT calculations in region ii with DFTB calculations (the "hybrid small"). In this case, all molecules except the charged molecule will be treated with DFTB. A full DFTB treatment of even the charge carrying sites completes the comparison of the calculations with explicit polarons ("semi-empirical"). Simulations within the simpler (much faster, but less precise) approach where the whole system is equilibrated without explicit additional charges ("polarization model") are performed within both the full DFT and the full DFTB approach in all regions i, ii, and iii as depicted in Figure 3b.

Energy disorder is calculated in the manner presented below. It contains all electronic contributions to disorder in the system, including polarization of the environment, the response, which is assumed to occur instantaneously. The reorganization energy λ, on the other hand, contains slow ionic relaxations. For the polaron method, a number of about 80 charged sites is explicitly calculated leading to a number of about 400 pairs and energy differences. The total energy differences of charged and uncharged equilibrated sites are used for the calculation of energetic disorder with the following equation.

$$\sigma = \sqrt{\frac{1}{2(N_{\text{pairs}} - 1)} \sum_{\text{pairs}} (\Delta E_{\text{total,charged}} - \Delta E_{\text{total,uncharged}})^2} \quad (3)$$

DOI: 10.1021/ct501023n
J. Chem. Theory Comput. 2015, 11, 560−567

Table 1. Applicability of the Formulation of our QM/QM Approach, i.e. the Hybrid DFT/Semi-empirical Quantum Patch Method Is Tested with the Following Five Partitioning Schemes for a Number of Systems[a]

		full QM	QM one shell only	hybrid large	hybrid small	semiempirical
Charged molecule	self-consistent	DFT	DFT	DFT	DFT	DFTB
12 Å environment		DFT	DFT	DFT	DFTB	DFTB
25 Å environment		DFT		DFTB	DFTB	DFTB
60 Å environment	static	DFT		DFTB	DFTB	DFTB

[a]For the definition of the methods, see the text.

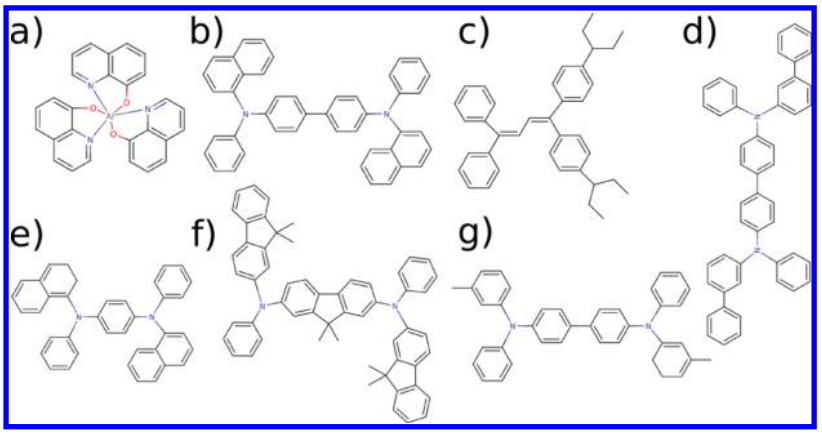

Figure 4. Chemical formulas of the seven organic molecules investigated here. (a) Alq_3,[46−50] (b) α-NPD,[46,50] (c) DEPB,[52] (d) mBPD,[53,54] (e) NNP,[55] (f) pFFA,[51] and (g)TPD.[46,49,52,56,57] In the references, charge carrier mobilities were measured.

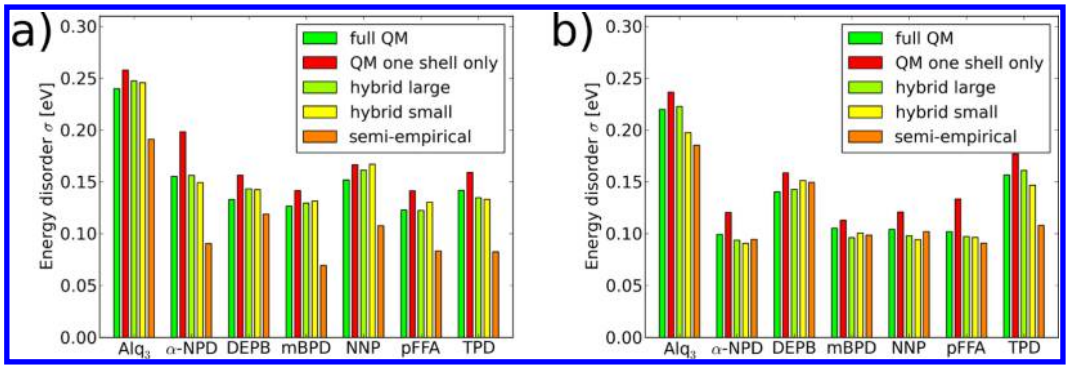

Figure 5. Energy disorder parameters for (a) holes and (b) electrons of the materials test set comprising seven different materials. The used methods are fully described in the text. In order to reproduce the results of the full QM reference method, the hybrid large method is found to be most appropriate.

In the polarization method, only the energies of the frontier HOMO and LUMO orbitals are used. Here, eq 4 is used.

$$\sigma = \sqrt{\frac{1}{2(N_{\text{pairs}} - 1)} \sum_{\text{pairs}} \Delta E_{\text{HOMO/LUMO}}{}^2} \tag{4}$$

The details of the procedure were presented in ref 28.

All DFT calculations were performed using TURBOMOLE package[30] with the hybrid B3-LYP functional[43] and a def2-SV(P) basis set.[44] The DFTB calculations were completed with the DFTB2 version[34] from the DFTB suite of models[45] using the mio-parameter set.[34]

RESULTS AND DISCUSSION

In order to test the validity of the QM/QM quantum patch protocols to compute the carrier mobility in organic semiconductors, we tested five different quantum patch protocols as defined in Table 1 in Methods. For each protocol, we have calculated the energy disorder parameters[28] for seven widely studied materials, namely tris(8-hydroxyquinolinato)aluminum (Alq_3), N,N′-bis(1-naphthyl)-N,N′-diphenyl-1,1′-biphenyl-4,4′-diamine (α-NPD), 1,1-bis(4,4′-diethylaminophenyl)-4,4-diphenyl-1,3,butadinene (DEPB), N4,N4′-di(biphenyl-3-yl)-N4,N4′-diphenylbiphenyl-4,4′-diamine (mBPD), N1,N4-di(naphthalen-1-yl)-N1,N4-diphenylbenzene-1,4-diamine (NNP), N,N′-bis-[9,9-dimethyl-2-fluorenyl]-N,N′-diphenyl-9,9-dimethylfluorene-2,7-diamine (pFFA), and N,N′-diphenyl-N,N′-bis(3-methylphenylene)-1,1′-diphenyl-4,4′-diamine (TPD) (see Figure 4). These materials cover a wide range of zero-field hole mobilities, ranging from 1.2×10^{-10} $cm^2/(V\ s)$ for Alq_3[46−50] to 7.6×10^{-4} $cm^2/(V\ s)$ for pFFA.[51]

The results of the various protocols are shown in Figure 5. The "full QM" calculations serve as the reference calculations. The "QM one shell only" uses only one neighbor shell of polarized molecules in the environment and all the deviations, more precisely the obvious overestimate, can be attributed to finite size of the polarizable shell. Full equilibration of the medium cannot take place resulting in too large energy

DOI: 10.1021/ct501023n
J. Chem. Theory Comput. 2015, 11, 560−567

Table 2. Comparison of the Energy Disorder Parameters for the Polaron II Method Performed on the DFT Level (Full QM as well as QM One Shell Only), Hybrids of DFT and DFTB Approaches (Hybrid Small and Hybrid Large), and DFTB (Semi-empirical)

	Energy Disorder σ (eV)									
	holes					electrons				
	full QM	QM one shell only	hybrid large	hybrid small	semi-empirical	full QM	QM one shell only	hybrid large	hybrid small	semi-empirical
Alq_3	0.240	0.258	0.247	0.246	0.191	0.220	0.236	0.223	0.197	0.185
α-NPD	0.155	0.198	0.156	0.149	0.090	0.099	0.120	0.093	0.091	0.094
mBPD	0.133	0.156	0.143	0.142	0.119	0.140	0.159	0.143	0.151	0.150
DEPB	0.126	0.142	0.130	0.131	0.069	0.105	0.113	0.096	0.101	0.099
NNP	0.152	0.167	0.161	0.167	0.108	0.104	0.121	0.098	0.094	0.102
pFFA	0.123	0.141	0.122	0.130	0.083	0.102	0.133	0.097	0.096	0.091
TPD	0.142	0.159	0.135	0.133	0.082	0.157	0.177	0.161	0.147	0.108

differences and, thus, too strong energy disorder. Therefore, we introduce the "hybrid large" method, where the first coordination shells of molecules around the charged centers are calculated in DFT as well as the charged molecule itself. This method leads to very accurate energy disorder parameters for all materials in the set, while providing almost an order of magnitude CPU-time cost reduction compared to the full QM method (see Figure 7). In the "hybrid small" quantum patch method only the charged molecules are treated on DFT level. The neighboring self-consistently evaluated and polarized molecules along with the static molecules are all calculated in DFTB. The energy disorder calculated with this method is in almost all of the cases fairly close to the results from the "full QM" method with the deviations varying between −10% and +10% for Alq_3 (electrons) and NNP (holes), respectively. But, as charge carrier mobility is very sensitive to changes in energy disorder ($\mu \propto \exp(-c(\beta\sigma)^2)$),[9,19−21] this will still produce considerable errors in the mobility predictions and therefore is not robust enough for a systematic predictive method with ambitions of performing in silico screening of novel organic semiconductors.

Finally, the "full semi-empirical" calculations, systematically underestimate the energy disorder for holes, while yielding results, which are within 6% of the "full QM" results for electrons for alpha-NPD, mBPD, and NNP. One possible explanation could be the minimal basis set deployed within the DFTB method, which leads to underpolarization.[58] This implies, again, that the energies of the charged states of molecules cannot be predicted reliably with exclusive use of semiempirical methods within quantum patch algorithm. As an example, the deviation of energy differences between DFT and DFTB for 300 Alq_3 pairs is ±0.142 eV for positively charged molecules and ±0.108 eV for negatively charged molecules leading to large discrepancies between "full QM" and "semi-empirical" energy disorder. All numbers are provided in Table 2.

In order to compare the results from the polaron method with a faster equilibration method, we introduced the polarization quantum patch method, based on neutral sample equilibration without explicit additional charges. The results for this method are shown in Table 3. The purely semiempirical method as implemented in quantum patch algorithm is producing deviations when compared to the full QM, which vary between +12% for α-NPD electron disorder and −30% for TPD hole disorder. The inherent requirements of this method do not allow for a large CPU timesaving and speed-up by splitting the system into DFT and DFTB parts as was achieved in the polaron method. For this reason, no hybrid approaches were pursued within the polarization approach.

Table 3. Comparison of the Energy Disorder Parameters for the Polarization Method Performed on the DFT Level of Theory (Full QM) and DFTB (Semi-empirical)[a]

	energy disorder σ (eV)			
	full QM		semi-empirical	
	holes	electrons	holes	electrons
Alq_3	0.224	0.239	0.212	0.204
α-NPD	0.144	0.111	0.107	0.125
mBPD	0.130	0.131	0.140	0.140
DEPB	0.109	0.120	0.083	0.128
NNP	0.135	0.112	0.138	0.116
pFFA	0.112	0.102	0.089	0.109
TPD	0.129	0.157	0.093	0.155

[a]Deviations of up to 30% in energy disorder depending on the used calculation methods along with no simple way to "hybridize" the polarization approach with obvious CPU-time savings made usage of DFTB within this approach unfavorable.

To put our results in the right context we have illustrated the extreme sensitivity of the charge carrier mobility on positive or negative deviations in the energy disorder in the model shown in Figure 6. The exponential dependence of the mobility on the energy disorder strength results in tremendous changes in the charge carrier mobility even for rather small errors in the energy disorder.

We compared the computational requirements of the different protocols; the results are shown in Figure 7. One DFT calculation of a charged molecules takes 15 min of CPU-time on a 2.6 GHz Intel Xeon processor E5-2670 (Sandy Bridge) including pre- and postprocessing of a charged molecule where a B3-LYP[43]/SV(P)[44] level of theory was used as implemented in TURBOMOLE[30] and 6 min for an uncharged molecule on the same level of theory. The corresponding calculations within DFTB take on average 4 s per molecule. We typically use seven self-consistency steps in the quantum patch method, 100 charged centers, each of them surrounded by 100 molecules which are self-consistently re-evaluated in each iteration cycle. For the hybrid large method, 12 of these 100 molecules are treated with DFT and the rest in DFTB. For simplification, any additional preparation steps and precalculations of the system along with any dimer calculations for the electronic couplings were not taken into account. The full QM method in this calculation needs 14 210 CPU-h. The hybrid large method gives the most accurate results, as it

DOI: 10.1021/ct501023n
J. Chem. Theory Comput. 2015, 11, 560−567

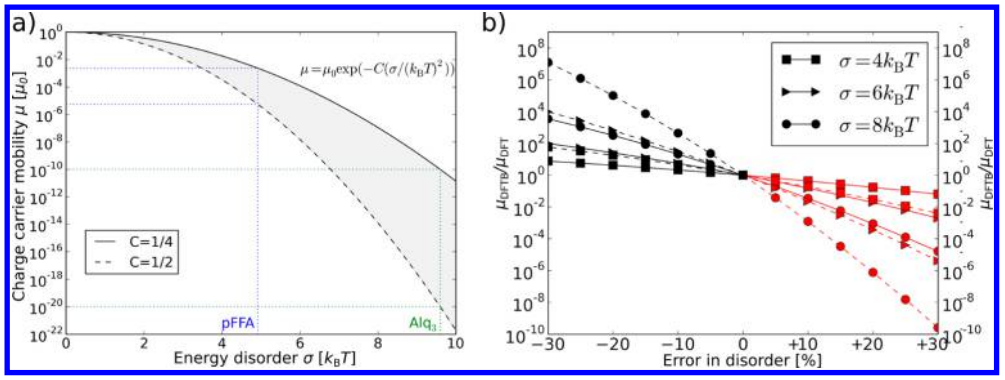

Figure 6. (a) Exponential dependence of the charge carrier mobility on energy disorder for $C = 1/2$ and $C = 1/4$ (see eq 2). As an example, disorder strengths for two specific materials are shown in the plot. (b) Positive and negative shifts up to ±30% of the energy disorder, the largest deviation between DFT and DFTB, lead to changes in charge carrier mobility (μ_{DFTB}/μ_{DFT} presented on the *y*-axis) of between 5 and 10 orders of magnitude, depending on the prefactor *C*. The changes grow larger as eq 2 becomes more sensitive for the larger *C* parameter 1/2 (dashed lines) and for larger energy disorder σ (circles).

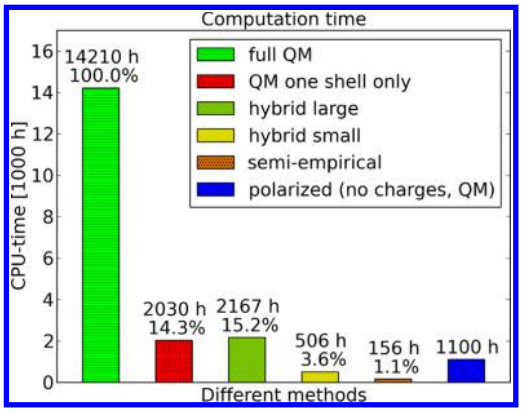

Figure 7. Comparison of the computational effort for the presented methods. The most accurate method (see Figure 5) "hybrid large" is reducing the computational cost by over 80% (almost an order of magnitude) without any significant loss of precision.

reduces the full QM effort to 15.2% or 2167 CPU-h. The hybrid small method reduces the computational effort to 3.6% or 506 CPU-h, whereas the full semiempirical method requires only 156 h (1.1% of the full DFT CPU-time). As a comparison, the last column shows the computational effort for the polarization quantum patch method (explained above). In order to calculate the energy disorder from total energies rather than orbital energies, the total energies of uncharged molecules in equilibrated environment are needed as reference values (for details, see ref 28). The most accurate hybrid large Polaron approach is less than factor two more expensive than the affordable (but not as precise) Polarization model, which clearly brings the Polaron approach on the map of methods, which are readily available for in silico materials prescreening.

To better understand where, why, and how the "hybridizing" of the quantum patch method works, we did a direct comparison between DFT and DFTB calculations for a few relevant quantities. Namely, for neutral Alq_3 molecules in vacuum we obtained typical dipole moments of $d = 4.9 \pm 0.9$ D, while the dipole moments in DFTB of the same set of molecules were 4.2 ± 0.8 D, which is comparable. For the positively charged Alq_3 molecules in vacuum the center of charge differs by only 0.36 ± 0.17 Å between DFT and DFTB, indicating method independent electronic structure, as different orbital structure in Alq_3 would almost certainly move the charge center to another ligand, resulting in differences of several angstroms at the very least. Further, the total energy difference between the neighboring molecules (dimers), as displayed in eq 3 is the main information used by the quantum patch method to obtain the energy disorder of a morphology. Thus, this difference is expected to be independent of the calculation method, or the difference of the total energy differences within each molecular dimer, coming from the calculation method ($\delta\Delta E_{calc.method}$), is expected to be very small. However, for positively charged Alq_3 molecules, this difference is ±0.43 eV clearly indicating that while DFTB seems to capture relevant physics of the charge density very well, there are discrepancies in the evaluation of the dimer energy differences. As our primary interest is the reproduction of the full DFT results, these observations justify the "onion" type model, where a number of radial cutoffs for DFT (especially the inner part where the total energies are relevant) and DFTB (focusing on the outer shell where the dominating interaction is between the central charge monopole and the local charge dipole) is respectively used.

CONCLUSIONS

We have recently developed a fully self-consistent QM embedding approach to compute environmental effects on polarons and other species in small molecule based organic semiconductors. This first principle approach has the advantage of being independent of force fields and therefore empirical parametrization. The method is highly parallelizable and does not need DFT calculations containing large parts of the morphology at once due to the reduction to single interacting molecules. This partitioning of the morphology further allows for the potential employment of different (MP2, CC2, etc.) computation methods for the central molecule. The electrostatic interaction between molecules is always mapped to the interaction with an external electrostatic potential represented by partial charges of the respective molecule. Therefore, the model does not contain constraints that must be extrapolated to zero.

However, to yield statistically meaningful results the quantum patch method must be applied to large samples, resulting in large computational costs. In this investigation we have presented a QM/QM quantum patch method as a viable extension of the original quantum patch method. Fast semiempirical density functional theory based tight binding

DOI: 10.1021/ct501023n
J. Chem. Theory Comput. 2015, 11, 560−567

calculations are combined with density functional methods and compared to the previous results. We find an optimal choice of parameters, where the calculations are accelerated by up to 1 order of magnitude without any significant change in the final computed energy disorder parameters for seven different materials. Accelerating the time-limiting quantum chemical step of our multiscale workflow may enable more accurate and efficient disordered organic semiconductors simulations on readily available computational hardware. Development of such methods is a significant step toward precise, efficient, and robust in silico materials screening. The applicability of the method is by no means limited to the charge carrier mobilities presented here but may be also used for studies of exciton diffusion lengths, charge transfers in guest−host systems, etc.

AUTHOR INFORMATION

Corresponding Author

*E-mail: wolfgang.wenzel@kit.edu. Phone: +49 721 608 26386.

Notes

The authors declare no competing financial interest.

ACKNOWLEDGMENTS

This work was funded by the STW-DFG MODOELED project. We thank Christian Lennartz (BASF, Germany), Falk May (BASF, Germany), Peter Bobbert (TU Eindhoven, The Netherlands), and Reinder Coehoorn (Philips Research Laboratories, Eindhoven, The Netherlands) for fruitful discussions. We acknowledge support by Ivan Kondov (SCC, KIT, Germany), Gesa Lüdemann, and Kai Welke (IPC, KIT, Germany). This work was supported by the FP-7 e-infrastructure project MMM@HPC, the PRACE6 and PRACE DECI8 projects. The calculations were performed using computational resource bwUniCluster funded by the Ministry of Science, Research and Arts and the Universities of the State of Baden-Württemberg, Germany, within the framework program bwHPC. Furthermore, we thank the Carl-Zeiss Foundation for funding the project Multiskalen Modellierung elektronischer Eigenschaften von Materialien in der organischen Elektronik.

REFERENCES

(1) Coropceanu, V.; Cornil, J.; da Silva Filho, D. A.; Olivier, Y.; Silbey, R.; Brédas, J.-L. Charge Transport in Organic Semiconductors. *Chem. Rev.* **2007**, *107*, 926−952.

(2) Nelson, J. Organic Photovoltaic Films. *Curr. Opin. Solid State Mater. Sci.* **2002**, *6*, 87−95.

(3) Chua, L.-L.; Zaumseil, J.; Chang, J.-F.; Ou, E. C.-W.; Ho, P. K.-H.; Sirringhaus, H.; Friend, R. H. General Observation of N-Type Field-Effect Behaviour in Organic Semiconductors. *Nature* **2005**, *434*, 194−199.

(4) Kim, Y. W.; Kwak, W. K.; Lee, J. Y.; Choi, W. S.; Lee, K. Y.; Kim, S. C.; Yoo, E. J. 9.1:40 Inch Fhd Am-Oled Display with Ir Drop Compensation Pixel Circuit. *SID Symp. Dig. Tech. Pap.* **2009**, *40*, 85−87.

(5) Lee, M. H.; Seop, S. M.; Kim, J. S.; Hwang, J. H.; Shin, H. J.; Cho, S. K.; Min, K. W.; Kwak, W. K.; Jung, S. I.; Kim, C. S.; Choi, W. S.; Kim, S. C.; Yoo, E. J. 53.4: Development of 31-Inch Full-Hd Amoled Tv Using Ltps-Tft and Rgb Fmm. *SID Symp. Dig. Tech. Pap.* **2009**, *40*, 802−804.

(6) Hast, J.; Tuomikoski, M.; Suhonen, R.; Väisänen, K.-L.; Välimäki, M.; Maaninen, T.; Apilo, P.; Alastalo, A.; Maanineny, A. 18.1: Invited Paper: Roll-to-Roll Manufacturing of Printed Oleds. *SID Symp. Dig. Tech. Pap.* **2013**, *44*, 192−195.

(7) Sasabe, H.; Kido, J. Multifunctional Materials in High-Performance Oleds: Challenges for Solid-State Lighting†. *Chem. Mater.* **2010**, *23*, 621−630.

(8) Baranovskii, S. Theoretical Description of Charge Transport in Disordered Organic Semiconductors. *Phys. Status Solidi B* **2014**, *251*, 487−525.

(9) Bässler, H. Charge Transport in Disordered Organic Photoconductors a Monte Carlo Simulation Study. *Phys. Status Solidi B* **1993**, *175*, 15−56.

(10) Roichman, Y.; Preezant, Y.; Tessler, N. Analysis and Modeling of Organic Devices. *Phys. Status Solidi A* **2004**, *201*, 1246−1262.

(11) Coehoorn, R.; Pasveer, W.; Bobbert, P.; Michels, M. Charge-Carrier Concentration Dependence of the Hopping Mobility in Organic Materials with Gaussian Disorder. *Phys. Rev. B* **2005**, *72*, 155206.

(12) Baumeier, B.; May, F.; Lennartz, C.; Andrienko, D. Challenges for in Silico Design of Organic Semiconductors. *J. Mater. Chem.* **2012**, *22*, 10971−10976.

(13) May, F.; Al-Helwi, M.; Baumeier, B.; Kowalsky, W.; Fuchs, E.; Lennartz, C.; Andrienko, D. Design Rules for Charge-Transport Efficient Host Materials for Phosphorescent Organic Light-Emitting Diodes. *J. Am. Chem. Soc.* **2012**, *134*, 13818−13822.

(14) Kwiatkowski, J. J.; Nelson, J.; Li, H.; Bredas, J. L.; Wenzel, W.; Lennartz, C. Simulating Charge Transport in Tris (8-Hydroxyquinoline) Aluminium (Alq3). *Phys. Chem. Chem. Phys.* **2008**, *10*, 1852−1858.

(15) Lee, C.; Waterland, R.; Sohlberg, K. Prediction of Charge Mobility in Amorphous Organic Materials through the Application of Hopping Theory. *J. Chem. Theory Comput.* **2011**, *7*, 2556−2567.

(16) Cottaar, J.; Koster, L.; Coehoorn, R.; Bobbert, P. Scaling Theory for Percolative Charge Transport in Disordered Molecular Semiconductors. *Phys. Rev. Lett.* **2011**, *107*, 136601.

(17) Marcus, R. A. Chemical and Electrochemical Electron-Transfer Theory. *Annu. Rev. Phys. Chem.* **1964**, *15*, 155−196.

(18) (a) Marcus, R.; Sutin, N. *Biophys. Acta* **1985**, *811*, 265. (b) Marcus, R. A. *Angew. Chem., Int. Ed. Engl.* **1993**, *32*, 1111−1121.

(19) Pasveer, W. F.; Cottaar, J.; Tanase, C.; Coehoorn, R.; Bobbert, P. A.; Blom, P. W. M.; De Leeuw, D. M.; Michels, M. A. J. Unified Description of Charge-Carrier Mobilities in Disordered Semiconducting Polymers. *Phys. Rev. Lett.* **2005**, *94*, 206601.

(20) Novikov, S. V.; Dunlap, D. H.; Kenkre, V. M.; Parris, P. E.; Vannikov, A. V. Essential Role of Correlations in Governing Charge Transport in Disordered Organic Materials. *Phys. Rev. Lett.* **1998**, *81*, 4472−4475.

(21) Huber, D. L. Diffusion of Optical Excitation at Finite Temperatures. *J. Chem. Phys.* **1983**, *78*, 2530−2532.

(22) Mesta, M.; Carvelli, M.; de Vries, R. J.; van Eersel, H.; van der Holst, J. J. M.; Schober, M.; Furno, M.; Lüssem, B.; Leo, K.; Loebl, P.; Coehoorn, R.; Bobbert, P. A. Molecular-Scale Simulation of Electroluminescence in a Multilayer White Organic Light-Emitting Diode. *Nat. Mater.* **2013**, *12*, 652−658.

(23) Rodin, V.; Symalla, F.; Friederich, P.; Meded, V.; Danilov, D.; Poschlad, A.; Nelles, G.; von Wrochem, F.; Wenzel, W. A Generalized Effective Medium Model for the Carrier Mobility in Amorphous Organic Semiconducturs. *Phys. Rev. B*, submitted for publication.

(24) Cottaar, J. Modeling of Charge-Transport Processes for Predictive Simulation of Oleds. Ph.D. dissertation, Eindhoven University, Eindhoven, 2012.

(25) Coehoorn, R.; van Mensfoort, S. L. M. Effects of Disorder on the Current Density and Recombination Profile in Organic Light-Emitting Diodes. *Phys. Rev. B* **2009**, *80*, 085302.

(26) Rühle, V.; Junghans, C.; Lukyanov, A.; Kremer, K.; Andrienko, D. Versatile Object-Oriented Toolkit for Coarse-Graining Applications. *J. Chem. Theory Comput.* **2009**, *5*, 3211−3223.

(27) Difley, S.; Wang, L.-P.; Yeganeh, S.; Yost, S. R.; Voorhis, T. V. Electronic Properties of Disordered Organic Semiconductors Via Qm/Mm Simulations. *Acc. Chem. Res.* **2010**, *43*, 995−1004.

(28) Friederich, P.; Symalla, F.; Meded, V.; Neumann, T.; Wenzel, W. Ab Initio Treatment of Disorder Effects in Amorphous Organic

DOI: 10.1021/ct501023n
J. Chem. Theory Comput. 2015, 11, 560−567

Materials: Toward Parameter Free Materials Simulation. *J. Chem. Theory Comput.* **2014**, *10*, 3720−3725.
(29) Berendsen, H. J. C.; van der Spoel, D.; van Drunen, R. Gromacs: A Message-Passing Parallel Molecular Dynamics Implementation. *Comput. Phys. Commun.* **1995**, *91*, 43−56.
(30) Ahlrichs, R.; Bär, M.; Häser, M.; Horn, H.; Kölmel, C. Electronic Structure Calculations on Workstation Computers: The Program System Turbomole. *Chem. Phys. Lett.* **1989**, *162*, 165−169.
(31) Eichkorn, K.; Treutler, O.; Öhm, H.; Häser, M.; Ahlrichs, R. Auxiliary Basis Sets to Approximate Coulomb Potentials. *Chem. Phys. Lett.* **1995**, *240*, 283−290.
(32) Eichkorn, K.; Weigend, F.; Treutler, O.; Ahlrichs, R. Auxiliary Basis Sets for Main Row Atoms and Transition Metals and Their Use to Approximate Coulomb Potentials. *Theor. Chem. Acc.* **1997**, *97*, 119−124.
(33) Weigend, F. Accurate Coulomb-Fitting Basis Sets for H to Rn. *Phys. Chem. Chem. Phys.* **2006**, *8*, 1057−1065.
(34) Elstner, M.; Porezag, D.; Jungnickel, G.; Elsner, J.; Haugk, M.; Frauenheim, T.; Suhai, S.; Seifert, G. Self-Consistent-Charge Density-Functional Tight-Binding Method for Simulations of Complex Materials Properties. *Phys. Rev. B* **1998**, *58*, 7260.
(35) Porezag, D.; Frauenheim, T.; Köhler, T.; Seifert, G.; Kaschner, R. Construction of Tight-Binding-Like Potentials on the Basis of Density-Functional Theory: Application to Carbon. *Phys. Rev. B* **1995**, *51*, 12947−12957.
(36) Seifert, G.; Porezag, D.; Frauenheim, T. Calculations of Molecules, Clusters, and Solids with a Simplified Lcao-Dft-Lda Scheme. *Int. J. Quantum Chem.* **1996**, *58*, 185−192.
(37) Caleman, C.; van Maaren, P. J.; Hong, M.; Hub, J. S.; Costa, L. T.; van der Spoel, D. Force Field Benchmark of Organic Liquids: Density, Enthalpy of Vaporization, Heat Capacities, Surface Tension, Isothermal Compressibility, Volumetric Expansion Coefficient, and Dielectric Constant. *J. Chem. Theory Comput.* **2011**, *8*, 61−74.
(38) Wang, J.; Hou, T. Application of Molecular Dynamics Simulations in Molecular Property Prediction. 1. Density and Heat of Vaporization. *J. Chem. Theory Comput.* **2011**, *7*, 2151−2165.
(39) Neumann, T.; Danilov, D.; Lennartz, C.; Wenzel, W. Modeling Disordered Morphologies in Organic Semiconductors. *J. Comput. Chem.* **2013**, *34*, 2716−2725.
(40) Wang, J.; Wolf, R. M.; Caldwell, J. W.; Kollman, P. A.; Case, D. A. Development and Testing of a General Amber Force Field. *J. Comput. Chem.* **2004**, *25*, 1157−1174.
(41) Jakalian, A.; Bush, B. L.; Jack, D. B.; Bayly, C. I. Fast, Efficient Generation of High-Quality Atomic Charges. Am1-Bcc Model: I. Method. *J. Comput. Chem.* **2000**, *21*, 132−146.
(42) Jakalian, A.; Jack, D. B.; Bayly, C. I. Fast, Efficient Generation of High-Quality Atomic Charges. Am1-Bcc Model: Ii. Parameterization and Validation. *J. Comput. Chem.* **2002**, *23*, 1623−1641.
(43) Becke, A. D. A New Mixing of Hartree-Fock and Local Density-Functional Theories. *J. Chem. Phys.* **1993**, *98*, 1372−1377.
(44) Schafer, A.; Horn, H.; Ahlrichs, R. Fully Optimized Contracted Gaussian Basis Sets for Atoms Li to Kr. *J. Chem. Phys.* **1992**, *97*, 2571−2577.
(45) Gaus, M.; Cui, Q.; Elstner, M. Density Functional Tight Binding: Application to Organic and Biological Molecules. *Wiley Interdiscip. Rev.: Comput. Mol. Sci.* **2014**, *4*, 49−61.
(46) Naka, S.; Okada, H.; Onnagawa, H.; Yamaguchi, Y.; Tsutsui, T. Carrier Transport Properties of Organic Materials for El Device Operation. *Synth. Met.* **2000**, *111*, 331−333.
(47) Fong, H. H.; So, S. K. Hole Transporting Properties of Tris (8-Hydroxyquinoline) Aluminum (Alq3). *J. Appl. Phys.* **2006**, *100*, 094502−094502−5.
(48) Kepler, R.; Beeson, P.; Jacobs, S.; Anderson, R.; Sinclair, M.; Valencia, V.; Cahill, P. Electron and Hole Mobility in Tris (8-Hydroxyquinolinolato-N1, O8) Aluminum. *Appl. Phys. Lett.* **1995**, *66*, 3618−3620.
(49) Kalinowski, J.; Camaioni, N.; Di Marco, P.; Fattori, V.; Martelli, A. Kinetics of Charge Carrier Recombination in Organic Light-Emitting Diodes. *Appl. Phys. Lett.* **1998**, *72*, 513−515.
(50) Tse, S.; Kwok, K.; So, S. Electron Transport in Naphthylamine-Based Organic Compounds. *Appl. Phys. Lett.* **2006**, *89*, 262102−262102−3.
(51) Okumoto, K.; Shirota, Y. Development of New Hole-Transporting Amorphous Molecular Materials for Organic Electroluminescent Devices and Their Charge-Transport Properties. *J. Mater. Sci. Eng. B* **2001**, *85*, 135−139.
(52) Mori, T.; Sugimura, E.; Mizutani, T. Estimate of Hole Mobilities of Some Organic Photoconducting Materials Using the Time-of-Flight Method. *J. Phys. D: Appl. Phys.* **1993**, *26*, 452.
(53) Shirota, Y.; Okumoto, K.; Inada, H. Thermally Stable Organic Light-Emitting Diodes Using New Families of Hole-Transporting Amorphous Molecular Materials. *Synth. Met.* **2000**, *111*, 387−391.
(54) Okumoto, K.; Wayaku, K.; Noda, T.; Kageyama, H.; Shirota, Y. Amorphous Molecular Materials: Charge Transport in the Glassy State of N, N′-Di (Biphenylyl)-N, N′-Diphenyl-[1, 1′-Biphenyl]-4, 4′-Diamines. *Synth. Met.* **2000**, *111*, 473−476.
(55) Borsenberger, P.; Shi, J. Hole Transport in a Vapor Deposited Phenylenediamine Molecular Glass. *Phys. Status Solidi B* **1995**, *191*, 461−469.
(56) Stolka, M.; Yanus, J.; Pai, D. Hole Transport in Solid Solutions of a Diamine in Polycarbonate. *J. Phys. Chem.* **1984**, *88*, 4707−4714.
(57) Heun, S.; Borsenberger, P. A Comparative Study of Hole Transport in Vapor-Deposited Molecular Glasses of N, N′, N″, N‴-Tetrakis (4-Methylphenyl)-(1, 1′-Biphenyl)-4, 4′-Diamine and N, N′-Diphenyl-N, N′-Bis (3-Methylphenyl)-(1, 1′-Biphenyl)-4, 4′-Diamine. *Chem. Phys.* **1995**, *200*, 245−255.
(58) Kaminski, S.; Gaus, M.; Elstner, M. Improved Electronic Properties from Third-Order Scc-Dftb with Cost Efficient Post-Scf Extensions. *J. Phys. Chem. A* **2012**, *116*, 11927−11937.

DOI: 10.1021/ct501023n
J. Chem. Theory Comput. 2015, 11, 560−567